Appl Phys A (2013) 112:65–69
DOI 10.1007/s00339-012-7203-0

Applied Physics A
Materials Science & Processing

Laser tattoo removal as an ablation process monitored by acoustical and optical methods

Boris Cencič · Peter Gregorčič · Janez Možina · Matija Jezeršek

Received: 29 June 2011 / Published online: 5 September 2012

Abstract Strength of the laser–tissue interaction varies even within a single tattoo because of the inhomogeneous distribution of the tattoo pigment embedded in the skin. A monitoring system is therefore developed for simultaneous monitoring of the laser tattoo removal process based on acoustical and optical techniques. A laser-beam-deflection probe is used for measuring the acoustical signals accompanying the breakdown, and a CCD camera captures the level and the spatial distribution of the plasma radiation. Using these methods we examine the degree of excitation-pulse absorption within the pigment and the degree of the structural changes of the skin. A Nd:YAG laser with a top-hat beam profile, designed for tattoo removal, is used as the excitation source in our experiments. Special attention is given to structural changes in the skin, which depend on the applied fluence. Tattoo removal with multiple pulses is also analyzed. Experiments are made *in vitro* (skin phantoms) and *ex vivo* (marking tattoos on the pig skin). The presented results are important for the understanding and optimization of the process used in medical therapies.

1 Introduction

The intradermal tattoos embedded in human skin can be effectively removed by Q-switched lasers with light having wavelength in the visible and near-IR region [1]. Optical breakdown which takes place within the tissue [2–5] makes the tattoo removal a specific ablation process. The skin strongly scatters and weakly absorbs the laser light having 1064-nm wavelength. On the other hand, the black or blue tattoo pigments act as strong absorbers. Microscopic studies [6] show that the pigment is distributed in the tissue in aggregates of different sizes, unevenly distributed. Optical breakdown and plasma formation are induced at all fluences of clinical interest ($>1\ \mathrm{J\,cm^{-2}}$) due to the light absorption within the pigment particles. The expanding plasma couples the laser energy into the mechanical energy through an optodynamic process [7], which is beneficial for the pigment breakup. Moreover, during this process sufficiently high temperatures are reached for the chemical decomposition of the pigment to take place [8]. However, the highest fluences are limited by the skin damage caused by subsurface explosions and by the epidermal damage due to the absorption in the epidermis. Therefore, double pulses are sometimes used for the minimization of collateral effects [9] or to increase the overall fluence.

Because of the inhomogeneous distribution of the pigment in the skin, the strength of the laser-pulse–tissue interaction varies even within a single tattoo. Thus, real-time monitoring of the process is necessary to keep the fluences in the safe region during the entire clinical treatment. The main goal of this contribution is the real time analysis of the laser tattoo ablation. Here we use an experimental setup [10] that uses two measuring techniques: a fast laser-beam-deflection probe (LBDP) [11–13] and the photography with a charge-coupled device (CCD) camera in the spectral range between 400 and 900 nm. The LBDP detects the shock wave that originates from subsurface pigment explosions, while the camera visualizes the plasma which develops during the laser–pigment interaction. The experiments are performed *in vitro* (skin phantoms) and *ex vivo* (marking tattoos on pig

B. Cencič
Fotona d.d., Stegne 7, 1210 Ljubljana, Slovenia

P. Gregorčič · J. Možina · M. Jezeršek (✉)
Faculty of Mechanical Engineering, University of Ljubljana, Aškerčeva 6, 1000 Ljubljana, Slovenia
e-mail: matija.jezersek@fs.uni-lj.si

skin). The results of this study are important for the optimization of the process in medical therapies.

2 Experimental setup

The experimental setup is presented in Fig. 1. A Q-switched Nd:YAG laser, designed for laser tattoo removal [14] is used as an excitation source. It uses a 7-mirror articulated arm for delivering pulses having a top-hat profile, duration of 6 ns (FWHM), energies up to 2 J, beam diameter of 4 mm and wavelength of 1064 nm, which is strongly absorbed in black and dark blue tattoos. Trigger photodiode (PD-T) is used to detect the excitation-laser pulse.

The laser–pigment and the laser–tissue interactions are examined by acoustical and optical measuring methods. The acoustical analysis is performed using a laser-beam-deflection probe (LBDP) that detects shock waves induced by the optical breakdown in the pigment layer. CCD camera is employed as an optical method for recording the intensity and the spatial distribution of the plasma radiation.

Shock waves are formed during tissue irradiation when substantial thermal and mechanical transients are generated by nanosecond laser pulses [4]. They spread into the surrounding air and are detected by the LBDP, with He–Ne laser ($\lambda = 633$ nm) used as a probe-beam. The probe-beam-waist diameter after the lens (L) is 50 μm, with the beam-waist position aligned with the position of the excitation-laser–sample interaction, as schematically shown in Fig. 1. The distance between the sample and the probe-beam is 8 mm. When the shock-wave front crosses the probe-beam, it is deflected by the refractive-index gradient [11, 15]. These deflections are detected with a position-sensitive photodetector, i.e., a 100-MHz bipolar photodiode (PD-B). The photodiode signal is captured by a digital oscilloscope (OSC; LeCroy, 600-MHz Wave Runner 64MXi-A).

Plasma radiation is recorded with the CCD camera (Point Grey, FireFly MV, 640 × 480 pixels). The camera is triggered simultaneously with the laser flash-lamp, and the camera shutter is open for 10 ms, i.e., much longer than the duration of the plasma-light emission. A low-pass filter (Schott KG5 glass filter) with sufficient optical density is used in front of the camera lens to completely block the excitation-laser light.

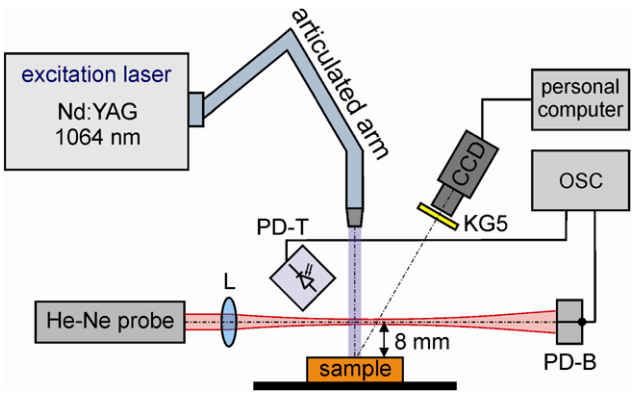

Fig. 1 A schematic presentation of the measuring setup

The experiments are made *in vitro* and *ex vivo*. For the *in vitro*, the skin phantoms are prepared on the glass slides. Three layers of collagen with thicknesses of 1, 0.2 and 1 mm, respectively, are used. The thinner, absorbing layer is mixed with Indian ink and is sandwiched between the thicker, transparent layers. Before experiments we have checked that the samples were homogeneous, i.e. without gas bubbles. The preparation of collagen gel is described in [16]. The *in vitro* samples are used to simulate the absorption within the pigment. In this case the scattering does not play an important role. The *ex vivo* experiments are performed using a fresh pig skin with tattoo marks.

3 Results and discussion

3.1 Bubble formation

Figure 2 shows images of the skin phantom and the pig skin after the single-pulse treatment. The figure implies that the bubbles remain in the tissue after the laser tattoo removal, a consequence of the high temperature developed during the laser–tattoo interaction inducing chemical decomposition of the pigment. The gaseous decomposition products remain in the tissue until they are eventually replaced by the extracellular liquid.

In vitro samples are used to prove the creation of long-lasting bubbles within the absorbing layer. Bleaching of the skin phantom within the irradiated area is clearly visible immediately after the single-pulse treatment (Fig. 2a). The image was taken with backlight illumination and small bubbles are evident in the bleached region. The dashed lines show the beam width of the excitation laser. A cross section of the same sample is shown in Fig. 2b to prove that the bubbles are presented in the ablated region. Due to the scatter of the laser light, the bubbles are seen to cover an area that is slightly larger than the illuminated area. Here we have used frontal in-line illumination, and the dashed line shows the left edge of the excitation beam (only a half of the illuminated area is shown in this case due to magnification). The treated absorbing layer appears brighter than the transparent layers due to the light scattering on the relatively coarse vacuolation structure (bubbles with diameter up to ∼0.5 mm). The layer also thickens due to the gaseous decomposition products.

Similar bubbles are observed also in *ex vitro* experiments. They can be seen in Fig. 2c, which shows the cross section of the pig skin after the single-pulse treatment. The dashed

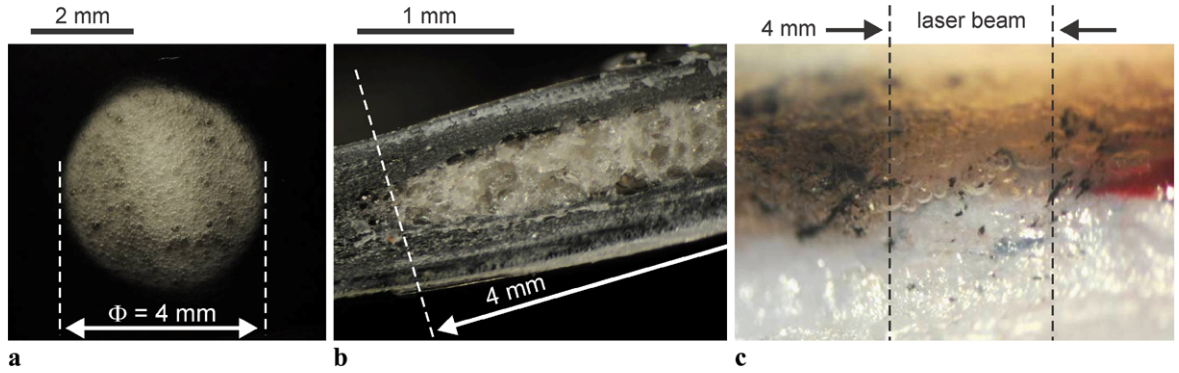

Fig. 2 Typical permanent bubbles formation after the single-pulse treatment ($F = 10\ \mathrm{J\,cm^{-2}}$). (**a**) Top view, and (**b**) cross section of the skin phantom. (**c**) Cross section of the pig skin

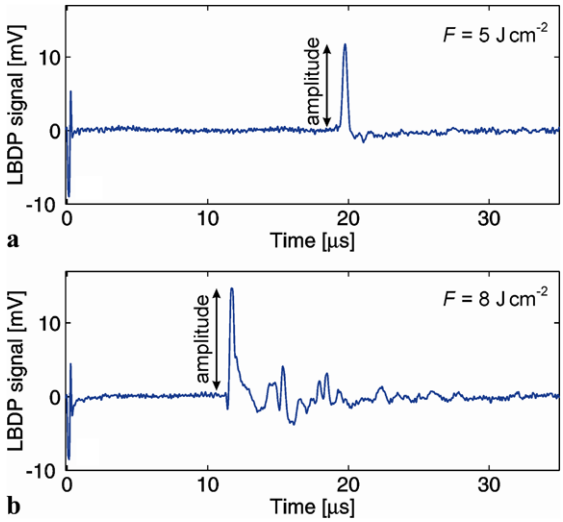

Fig. 3 Typical LBDP signals captured during *ex vivo* experiments using fluences of (**a**) $F = 5\ \mathrm{J\,cm^{-2}}$ and (**b**) $F = 8\ \mathrm{J\,cm^{-2}}$

lines in Fig. 2c indicate the region of the laser irradiance. The observation of bubbles indicates that they actually remain in the skin after the single-pulse treatment. This is important, since the presence of bubbles modifies the optical and mechanical properties of the skin, resulting in smaller efficiency of the second and further laser pulses, applied to the same area [10].

3.2 Analysis of the optodynamic signal

Figure 3 shows two typical optodynamic signals measured by LBDP during *ex vivo* experiments. Shock wave is generated during the laser–tattoo interaction and the strength of the interaction is determined from the detected shock waves. The shock-wave energy is related to the signal amplitude and the arrival time of the shock wave [17]. Our experiments [18] show that the shorter arrival time is measured for higher fluences. This is also clearly seen by the comparison of typical BDP signals shown in Fig. 3.

The signal in Fig. 3a is acquired during the irradiation of the sample with the fluence $F = 5\ \mathrm{J\,cm^{-2}}$ and its shape is consistent with the shape of the signal when the spherical shock waves are detected [11, 19]. On the other hand, the signal measured during the irradiation with highest fluence $F = 8\ \mathrm{J\,cm^{-2}}$ consists of several peaks with longer duration (see Fig. 3b). This can be explained as the arrival of several shock waves, which are generated due to the structural changes within and on the surface of the skin. The shape of the signal implies that the skin has suffered considerable and possibly excessive damage, i.e., specifically tissue vacuolation, perforation and particle ejection. Consequently, it can be used as an indication that the fluence is out of the safe region.

The amplitude of the LBDP signal (see Fig. 3) is correlated with the interaction strength [20]. The LBDP amplitude is therefore a suitable parameter to determine the strength of the laser–tissue interaction. Figure 4 shows the amplitude of the first LBDP peak as a function of the pulse fluence for *in vitro* (Fig. 4a) and *ex vivo* (Fig. 4b).

The dependence for the skin phantom samples (Fig. 4a) is expected—i.e., the interaction strength increases with the fluence. Contrary, the *ex vivo* results (Fig. 4b) are surprising since in the fluence range 2–6 $\mathrm{J\,cm^{-2}}$ the LBDP amplitude is practically independent of the fluence. At lower fluence levels, i.e., about 1 $\mathrm{J\,cm^{-2}}$, the relatively large variation in amplitude can be explained by the random nature of the threshold level for the optical breakdown. On the other hand, the large variation at fluences around 10 $\mathrm{J\,cm^{-2}}$ for *in vitro* and around 8 $\mathrm{J\,cm^{-2}}$ for *ex vivo* is explained by reaching the skin damage threshold, which is also a random phenomenon. Another cause of the large amplitude variation is the inhomogeneous distribution of the pigment, especially in the *ex vivo* samples (see Fig. 2c). However, the presented results show that the amplitude of the first peak is not a good measure of the laser–pigment interaction strength since a smaller and variable part of the laser energy is coupled into the fastest shock wave, which is detected as the first peak. Thus, more

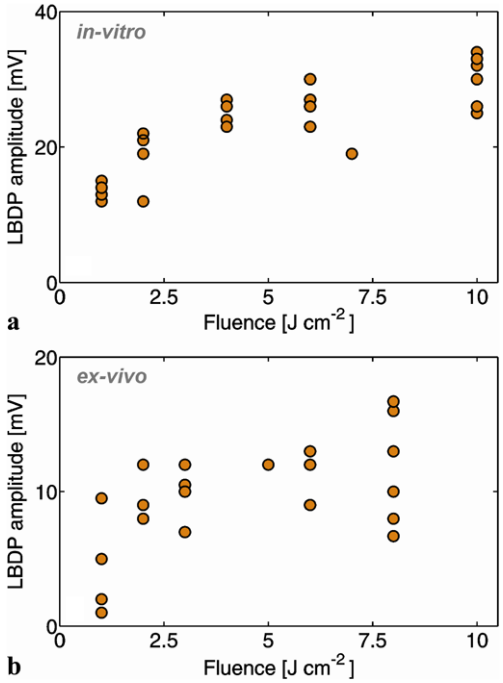

Fig. 4 The LBDP amplitude as a function of fluence measured for (**a**) skin phantom and (**b**) pig skin

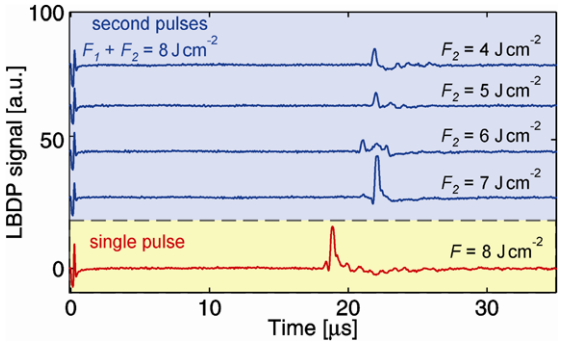

Fig. 5 Examples of the LBDP signals after (**a**) single pulse and (**b**) double pulse delivered to the same region of *ex vivo* samples in the time interval of 15 s. The cumulative fluence is $F = F_1 + F_2 = 8\ \mathrm{J\,cm^{-2}}$

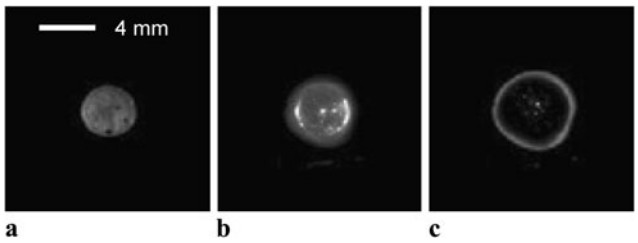

Fig. 6 Typical distribution of the plasma radiation on the skin phantoms for (**a**) a single pulse with low fluence $F = 2\ \mathrm{J\,cm^{-2}}$, (**b**) a first pulse with high fluence $F = 10\ \mathrm{J\,cm^{-2}}$, and (**c**) a second pulse with high fluence $F = 10\ \mathrm{J\,cm^{-2}}$

useful information is provided by the complex shape of the signal with several peaks (e.g., see Fig. 3b).

From the clinical experience it is known that the fluences near the interaction threshold value do not remove tattoos sufficiently. Therefore, for optimal results the fluence should be increased to reach values just below the damage threshold. Since the presented analysis enables the detection of the interaction-threshold as well as the threshold for the skin damage, it has a great potential to be implemented in the medical systems for the real-time monitoring of the process.

3.3 Double-pulse irradiation

The study of double-pulse irradiation was performed *ex vivo*. Here, two consecutive pulses are delivered to the same region. The cumulative fluence $F = F_1 + F_2$ for the first (F_1) and the second (F_2) pulse equals $F = 8\ \mathrm{J\,cm^{-2}}$ during all experiments. The value of the cumulative fluence was chosen as the maximum allowable fluence, determined from the analysis of the optodynamic signal.

The second pulse was delayed for 15 s. After that time the tissue temperature is less than 5 K higher comparing to the first one. This estimate was made by using the instantaneous point-source heat-diffusion equation [21]. Even smaller temperature difference with equal pulse fluence ($10\ \mathrm{J\,cm^{-2}}$) was measured by Milanič [22]. We assume that this residual thermal effect does not significantly change the optical properties of the illuminated tissue.

Figure 5 shows the LBDP signals for a single pulse (the bottommost signal; $F = 8\ \mathrm{J\,cm^{-2}}$) and for the second pulses from the following pulse combinations: $\{F_1 = 1\ \mathrm{J\,cm^{-2}}, F_2 = 7\ \mathrm{J\,cm^{-2}}\}$; $\{F_1 = 2\ \mathrm{J\,cm^{-2}}, F_2 = 6\ \mathrm{J\,cm^{-2}}\}$; $\{F_1 = 3\ \mathrm{J\,cm^{-2}}, F_2 = 5\ \mathrm{J\,cm^{-2}}\}$; and $\{F_1 = 4\ \mathrm{J\,cm^{-2}}, F_2 = 4\ \mathrm{J\,cm^{-2}}\}$.

It is clearly visible in Fig. 5 that the amplitudes of the second-pulse signal are considerably reduced, when the fluence F_1 of the first pulse exceeds $1\ \mathrm{J\,cm^{-2}}$ (the top three signals in Fig. 5). Moreover, in this case multiple peaks appear. We attribute this effect to the structural changes in the skin, made by the first pulse as it will be explained in the next subsection.

3.4 Analysis of the plasma radiation

Figure 6 shows plasma radiation for the *in vitro*. Plasma is detected at fluences over $1\ \mathrm{J\,cm^{-2}}$. When fluences in the range 2–4 $\mathrm{J\,cm^{-2}}$ are used, it appears spatially uniform due to the beam top-hat profile (see Fig. 6a). On the other hand, in the case of fluences over $10\ \mathrm{J\,cm^{-2}}$ hot spots appear (see Fig. 6b) due to slight beam-profile non-uniformities.

In the case of double-pulse illumination (see also Fig. 5), the intensity of the plasma radiation decreases strongly at the second pulse. Figure 6c shows the plasma radiation when the

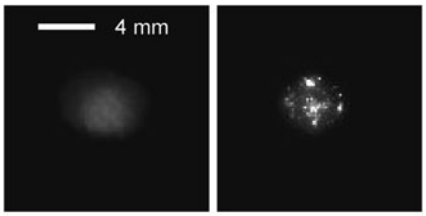

Fig. 7 Typical distribution of the plasma radiation on the pig skin for (**a**) low-fluence ($F = 2\ \mathrm{J\,cm^{-2}}$) and (**b**) high-fluence ($F = 10\ \mathrm{J\,cm^{-2}}$) single pulse

second pulse is delivered onto the same spot as the first one. In this case most of the plasma radiation is generated in the immediate vicinity, but not within the illuminated area. We assume that the bubbles generated by the previous pulse prevent the second pulse from reaching the remaining pigment within the illuminated area. Our experiments show that the pigment is not completely removed by the first pulse, therefore the shape and relatively smaller intensity of the plasma radiation during the second pulse can be attributed to (i) the partial bleaching of the pigment within the irradiated area, and (ii) the scattering of the second pulse by these bubbles (see also Fig. 2).

Figure 7 shows the plasma radiation for the *ex vivo* experiments. When the fluences in the range 2–4 $\mathrm{J\,cm^{-2}}$ are used on the pig skin, the plasma radiation appears very uniform (see Fig. 7a), since it originates in depth and is scattered strongly before it reaches the surface. The bright area has the shape of the tattoo because the beam size has exceeded the tattooed region. Figure 7b shows the plasma radiation when very high fluences, i.e., over 10 $\mathrm{J\,cm^{-2}}$, are applied on the pig skin. Under these conditions, the sharp and randomly distributed hot spots are observed even on untattooed skin. For monitoring purposes these spots are useful, since they originate on the skin surface and indicate possible epidermal damage.

4 Conclusion

We have shown that the presented acoustical and optical monitoring of the laser tattoo removal process can be used to obtain important information about (i) the ablation threshold of the tattooed and untattooed skin, (ii) the skin-damage threshold, and (iii) the structural changes of the skin.

The analysis of the double-pulse illumination has shown that the structural changes in the skin are caused by the first pulse. This happens even at lower fluences, when the fluence of the first pulse barely exceeds the ablation threshold. We have shown that the inefficiency of the second pulse is caused by the bubble formation in the tissue after the first-pulse treatment. Therefore, the multiple single-pulse therapies, which are performed in intervals that the skin needs to renew should be more effective than single multiple-pulse therapy.

Acknowledgements This work was supported by the EUREKA organization under the project "Intelligent Laser Sources in Dermatology and Aesthetic Medicine—iLUMEN".

References

1. K.M. Kent, E.M. Graber, Dermatol. Surg. **38**, 1 (2012)
2. R.R. Anderson, J.A. Parrish, Science **220**, 524 (1983)
3. S. Choudhary, M.L. Elsaie, A. Leiva, K. Nouri, Lasers Med. Sci. **25**, 619 (2010)
4. A. Vogel, V. Venugopalan, Chem. Rev. **103**, 577 (2003)
5. F.G. Perez-Gutierrez, S. Camacho-Lopez, G. Aguilar, J. Biomed. Opt. **16**, 115001 (2011)
6. J.E. Ferguson, S.M. Andrew, C.J.P. Jones, P.J. August, Br. J. Dermatol. **137**, 405 (1997)
7. J. Možina, J. Diaci, Appl. Phys. B **105**, 557 (2011)
8. V.K. Pustovalov, Laser Phys. **4**, 612 (1994)
9. A. Vogel, P. Schmidt, B. Flucke, Proc. SPIE **4257**, 184 (2001)
10. M. Jezeršek, L. Grad, T. Požar, B. Cencič, I. Bacak, J. Možina, Proc. SPIE **8092**, 809214 (2011)
11. J. Diaci, Rev. Sci. Instrum. **63**, 5306 (1992)
12. M. Villagran-Muniz, H. Sobral, R. Navarro-Gonzalez, Meas. Sci. Technol. **14**, 614 (2003)
13. R. Petkovšek, P. Gregorčič, J. Možina, Meas. Sci. Technol. **18**, 2972 (2007)
14. Z. Vižintin, M. Kažič, B. Cencič, L. Grad, D. Škrabelj, M. Lukač, Full spectrum tattoo removal laser system. Presented at IMCAS Conference, Paris, 2009
15. P. Gregorčič, R. Petkovšek, J. Možina, G. Močnik, Appl. Phys. A **93**, 901 (2008)
16. M. Milanič, B. Majaron, J. Biomed. Opt. **14**, 064024 (2009)
17. J. Diaci, J. Možina, J. Phys. IV **4**, 737 (1994)
18. B. Cencič, L. Grad, J. Možina, M. Jezeršek, J. Biomed. Opt. **17**, 047003 (2012)
19. J. Diaci, J. Možina, Appl. Phys. A **55**, 352 (1992)
20. G.M. Bilmes, D.J.O. Orzi, O.E. Martinez, A. Lencina, Appl. Phys. B **82**, 643 (2006)
21. W.M. Steen, J. Mazumder, *Laser Material Processing*, 4th edn. (Springer, London, 2010). Chap. 5.4.1
22. M. Milanič, B. Majaron, Proc. SPIE **8207**, 82070G (2012)